NANO MICRO small

Supramolecular Glyco-nanoparticles Toward Immunological Applications

Mingchang Lin, Yufei Zhang, Guosong Chen, and Ming Jiang*

Glyco-mimicking nanoparticles (glyco-NPs) with Förster resonance energy transfer (FRET) donor and acceptor groups formed via dynamic covalent bond of benzoboroxole and sugar from two complementary polymers are prepared. The glyco-NPs are proved to be quite stable under physiological conditions but sensitive to pH. So the glyco-NPs can be internalized by dendritic cells with integrity and nontoxicity and then dissociate within the acidic organelles. This particle dissociation is directly observed and visualized in vitro, for the first time via the FRET measurements and fluorescent microscopy. This feature makes controlled release of drug or protein by glyco-NPs possible, i.e., when model antigen Ovalbumin is loaded in the glyco-NPs, the released Ovalbumin in dendritic cells stimulates T cells more efficiently than the free Ovalbumin itself as a result of the enhanced antigen processing and presentation. Thus, the results enlighten a bright future of the glyco-NPs in immunotherapy.

1. Introduction

Mimicking the complex structures and various functions of cells has been a major and long-term target in self-assembly studies.[1] In this broad field, along with constructing the mimics to intracellular compartments (the organelles) and concerted enzymatic reactions wherein,[2] mimicking *glycocalyx*, i.e., the cell surface structure of a heavy layer of glycoprotein, glycolipid, and proteoglycan,[3] has drawn great attention due to the crucial role of the sugars on cell–cell interactions and cell–matrix interactions.[4] Our group and several others have achieved some of such mimics by using self-assembled glyco-containing macromolecules.[5] Very recently, we reported that our glycocalyx-mimicking nanoparticles (glyco-NPs) were able to activate macrophages by turning the immunosuppressive subtype to the immunoresponsive ones, which brought forth a great potential of such glyco-NPs in immunotherapy.[6]

Incorporation of the glyco-NPs into immunological cells is far from enough for immunotherapy. Generally, antigen-encapsulated nanoparticles need to be endocytosed into dendritic cells (DCs) first, which are the most effective antigen-presenting cell with the function of processing antigen material. Then subsequent steps are required, i.e., release of the antigen within the cell, presentation of the antigen on the cell surface, and then stimulating T cells for activation. Thus it is demanding to invent a new type of glyco-NPs as a nontoxic and intelligent antigen-vehicle, which could perform a lossless transfer of the preloaded antigen into cells and then release it within the organelles in DCs as designed. In our efforts to mimic glycocalyx, dynamic covalent bond has played a special role,[5a] which is featured by its dual natural characters: Depending on the environmental conditions, the bonds could be as labile as the noncovalent bonds or as inert as the covalent bonds.[7] As a derivative of phenylboronic acid, benzoboroxole (BOB) is employed in this work, particularly featured by its binding ability to nonreducing sugars at neutral condition, which broadens its targets to natural nonreducing saccharides.[8]

Dr. M. Lin, Y. Zhang, Prof. G. Chen, Prof. M. Jiang
State Key Laboratory of Molecular Engineering of Polymers
Department of Macromolecular Science
Fudan University
220 Handan Rd., Shanghai 200433, China
E-mail: guosong@fudan.edu.cn

DOI: 10.1002/smll.201501871

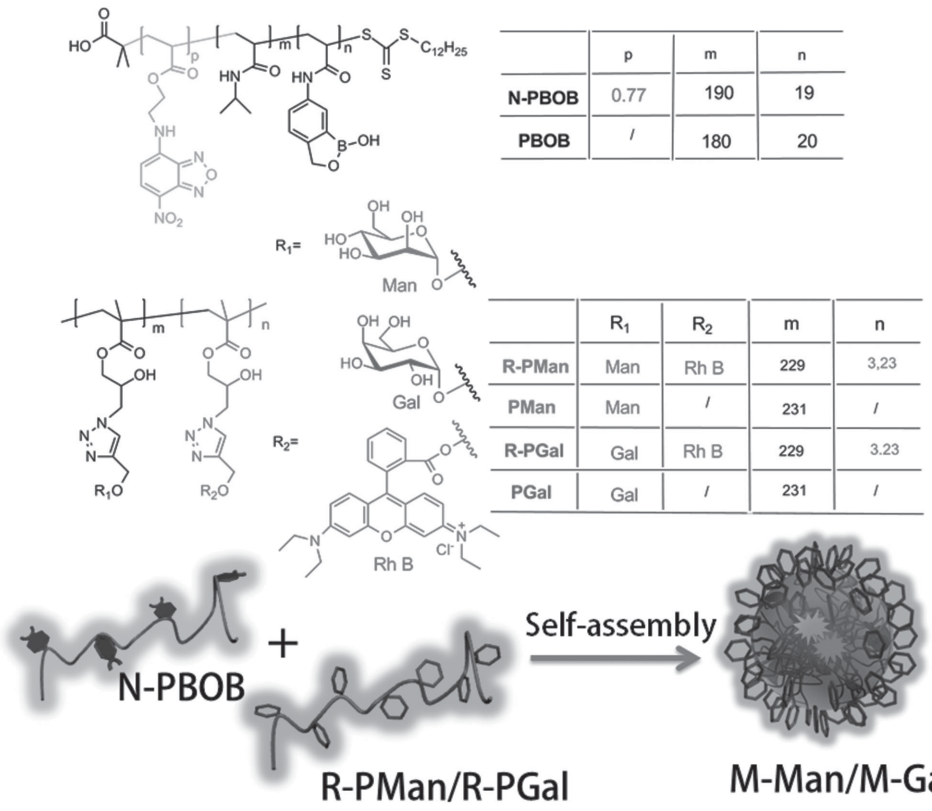

	p	m	n
N-PBOB	0.77	190	19
PBOB	/	180	20

	R_1	R_2	m	n
R-PMan	Man	Rh B	229	3,23
PMan	Man	/	231	/
R-PGal	Gal	Rh B	229	3.23
PGal	Gal	/	231	/

Scheme 1. Chemical structures of **PBOB**, and its FRET donor form **N-PBOB**, glycopolymer **PMan**, **PGal**, and their FRET acceptor forms **R-PMan**, **R-PGal**, respectively. The cartoon at the bottom represented the glyco-NP formation.

Herein, for the goal of exploring the possible immunological applications, a new type of supramolecular nanoparticles based on the dynamic covalent bond between BOB-containing polymer and glycopolymer was designed and prepared. The resultant glyco-NPs exhibited desirable properties: they were quite stable under physiological conditions, which ensured its endocytosis without being destroyed; while they were sensitive to pH, which enabled them to release the preloaded model antigen ovalbumin (OVA) in DCs due to their dissociation under the acidic organelles. Finally, therapeutic application of the responsive glyco-NP was demonstrated via the successful activation of T cells. Particularly, in the study, the success of using Förster resonance energy transfer (FRET) technique not only provided a simple way to evaluate the environmental responses of the particles but also for the first time, made their change within the organelles to be visualized. This work demonstrated the bright future of the glyco-NPs in cancer immunotherapy and vaccine development.

2. Results and Discussion

2.1. Design and Formation of Glyco-NPs

It is known that DCs have sugar-specific recognition receptors, i.e., mannose receptor (MR, CD206) to α-mannopyranoside (Man) and macrophage galactose lectin (MGL, CD301) to α-galactopyranoside (Gal). Herein, two corresponding polymers **PMan** and **PGal** with the same backbone, same molecular weight (M_w) and polydispersity index (PDI) containing respective monosaccharide stereoisomers, were synthesized[9] and employed (**Scheme 1**). Copolymer **PBOB** composed of *N*-isopropylacrylamide (NIPAm) and BOB was prepared according to our previous procedure.[9] For FRET studies, fluorescent donor 7-nitro-2,1,3-benzoxadiazole (NBD) and acceptor rhodamine B (RhB) were attached to **PBOB** and glycopolymers via copolymerization and post-polymerization modification, generating **N-PBOB** (Scheme 1 and Figure S2, Supporting Information) and **R-PMan**/**R-PGal** (Scheme 1 and Figure S3, Supporting Information), respectively[9] (preparation and characterization details of these polymers are in the Supporting Information, Figures S1–S7).

Mixing glycopolymers and **PBOB** in water at a low concentration (in most cases, 0.25 mg mL^{-1}) gave dramatic increases of the light scattering signals (I_s/I_0) and hydrodynamic radius $\langle R_h \rangle$, which indicated the formation of self-assembled nanoparticles due to the dynamic covalent bonding between the sugar and BOB species (Figure S8, Supporting Information). As shown in Table S1 of the Supporting Information, the composition of weight ratio 1:1 (glycopolymer: **PBOB**, molar ratio 2.93:1 calculated as monosaccharide: BOB) was selected to prepare glyco-NPs in this study. Different from the classical assembled nanoparticles from amphiphilic copolymers, in the glyco-NPs both **PBOB**, in which NIPAM units are dominant, and the glycopolymer kept hydrophilic. So in the nanoparticles, there is no clear core–shell structure. The formation of the nanoparticles

DOI: 10.1002/smll.201501871

was driven by the BOB-based dynamic bonds, which formed hydrophobic cross-linkers. This is very similar to the formation of nanoparticles of interpolymer complex due to hydrogen bonding, which has been intensively studied.[10] The current nanoparticles tend to have glyco-unit enriched on the surface because of its strong hydrophilicity than the other species. This was confirmed by the ^{1}H NMR data for the obtained glyco-NPs in D_2O where sugar units presented much stronger signals than those in the backbone and the isopropyl group of PNIPAm (Figure S9 and Table S2, Supporting Information).

2.2. FRET of Glyco-NPs

To monitor the stability and possible dissociation of glyco-NPs both in solution and in vitro, FRET of the glyco-NPs was studied by introducing the chromophores NBD and RhB into **PBOB** and the glycopolymers, respectively. NBD as a donor and RhB as a acceptor form a well-known FRET pair.[11] After attaching the chromophores into the polymer chains, this pair kept its FRET character well, as evidenced by the large overlap between the emission spectrum of **N-PBOB** and the excitation spectra of **R-PGal** and **R-PMan** (Figure S10, Supporting Information). In the FRET study, the ratio of the emission intensity at 587 nm of RhB to that of NBD at 538 nm (I_{587}/I_{538}) was evaluated. As shown in **Figure 1**a, when **N-PBOB** and **R-PGal** were mixed at an equal amount, FRET was so efficient that even no NBD emission at 538 nm was detected (Figure S11a, red line, Supporting Information). This was not suitable for the further study. Thus I_{587}/I_{538} was measured for a series of blended solutions composed of **PBOB**, **R-PGal,** and **PGal**, where **PGal** without the acceptor RhB was used to "dilute" RhB in the glyco-NPs (Figure S11b, Supporting Information). Obviously I_{587}/I_{538} decreased with increasing the proportion of the inert **PGal**. Finally, the composition of **N-PBOB**: **R-PGal**: **PGal** being 1:0.5:0.5, leading to I_{587}/I_{538} around 2.0 was selected. It is worth to mention that, as the emission spectra of PBOB were rather broad as shown in Figure S11a of the Supporting Information, the ratio of I_{587}/I_{538} of **PBOB** itself was around 0.69. Thus we think that if glyco-NPs give a low I_{587}/I_{538} around 1.0, they could be regarded as dissociated ones.

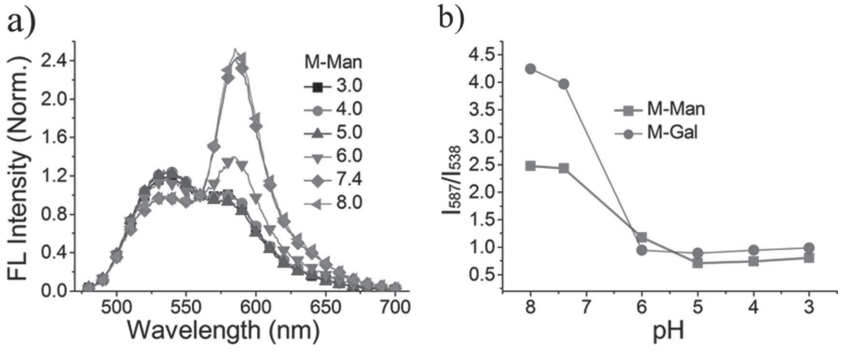

Figure 1. a) Normalized fluorescent intensity of **M-Man** at different pH. b) I_{587}/I_{538} of **M-Gal** and **M-Man** at different pH. Excitation wavelength: 466 nm. Measurements were performed after 30 min sonication.

2.3. Stability and Response of Glyco-NPs to Environmental Stimuli

For our final target of the immune application of the glyco-NPs, their responses to a series of stimuli including glucose, oxidents, temperature, and pH, which maybe met in physiological conditions, are the basic characters we concern first. The response of glyco-NPs to glucose was observed by monitoring the FRET ratio. Addition of glucose, a competitive sugar to the solutions of glyco-NPs, would generally cause a FRET ratio decrease as a result of the dissociation of the dynamic interactions between BOB and the sugar moieties and then dissociation of glyco-NPs. However, the degree of bond dissociation largely depends on concentration of the additional glucose (Figure S12, Supporting Information). Specifically, at a relative low concentration, e.g., 5 mg mL^{-1}, I_{587}/I_{538} value for **M-Man** and **M-Gal** were 2.7 and 1.8, respectively, this meant that the two component chains still formed tight complex, in other words, integration of the glyco-NPs remained. When the glucose concentration increased to a quite high range of 20–50 mg mL^{-1}, **M-Man** still kept stable, as its I_{587}/I_{538} was around 2.0 while **M-Gal** dissociated as the ratio decreasing to around 1.0. This conclusion of a large excess of glucose making dissociation of the dynamic bonds from **PGal** but not **PMan** is understandable as we demonstrated previously, that the strength of the bonding is in the order of **PMan** > **PGal**.[9] We noticed that the glucose concentration in blood is only around 0.8–1.2 mg mL^{-1}, so no doubt both of **M-Man** and **M-Gal** would keep stable under such a low glucose concentration.

Very similarly, according to DLS data, although high concentration of H_2O_2 (10×10^{-3} M) would induce the dissociation of both of **M-Man** and **M-Gal** (Figure S13a and details in the Supporting Information), at the concentration of H_2O_2 in the physiological condition (e.g., 3.3–109.6×10^{-6} M in human urine),[12] the glyco-NPs are quite stable (Figure S13b, Supporting Information). However, corresponding FRET estimation for the oxidant effect could not be performed due to the interference of H_2O_2 to the chromophores.

PBOB was composed of both NIPAm and BOB units so its response in the glyco-NPs to temperature was expected. As shown in Figures S14a and S15 of the Supporting Information, when temperature increased to over 37 °C, the FRET ratio of **M-Man** and **M-Gal** were 2.3 and 1.7, respectively, indicating that both of them were stable at the elevated temperatures. More significantly, even at 50 °C, FRET ratio of **M-Man** was as high as 2.0. The stability of glyco-NPs against temperature was also supported by DLS data. As shown in Figure S14b of the Supporting Information, $\langle R_h \rangle$ of **M-Man** remained constant during heating, although I_s/I_0 slightly increased, which might be caused by the collapse of PNIPAm segments inside **M-Man**. **M-Gal** showed similar phenomenon as shown in Figure S16 of the Supporting Information. It was not surprising to find that increasing temperature

DOI: 10.1002/smll.201501871

did not induce dissociation of the nanoparticles because the temperature-induced aggregation of the PNIPAm segments took place within the nanoparticles, which in fact was stabilized by the surface-rich sugar units.

PH response of the glyco-NPs was measured by FRET in buffer. When the solution pH was decreased slowly from 8.0 to 3.0, the fluorescent spectra of **M-Man** and **M-Gal** changed obviously (Figure 1a and Figure S17, Supporting Information). The calculated FRET ratio I_{587}/I_{538} from the spectra was plotted against pH in Figure 1b. An abrupt decrease of I_{587}/I_{538} in a pH range from 7.0 to 6.0 was observed for both of the glyco-NPs reaching a rather low value of 1.0, indicating dissociation of the starting glyco-NPs. This pH-induced dissociation of the nanoparticles is obviously fully in accordance with our previous conclusion that the dynamic bonding breaks at pH around 6.[9] Unfortunately, due the low solubility of **PBOB** under acidic condition in DLS measurement, the corresponding data could not be collected.

Summarizing the results of the responses to the stimuli of the glyco-NPs, one would find that the performance of the glyco-NPs very benefits their further study in immune applications: the stability against additional sugar and oxidant and temperature increase as provided in physiological conditions ensures that the particles would keep their integrity when they are uptaken by cells; The fast and robust response of the nanoparticles to pH is promising for them to release the preloaded antigen in the low pH organelles.

2.4. Colocalization and pH-Response of Glyco-NPs in DCs

It is well known that when the model antigen OVA is phagocytized by DCs, the protein is digested into small peptides by enzymes in lysosome, and then DCs will present these antigenic peptides on cell surface by coupling with major histocompatibility complex (MHC) molecules. This process is called antigen presentation. T cells can only recognize antigenic peptides displayed on the surface of DCs, and then differentiate into activated T cells. Thus the effective antigen presentation is a key step to cancer immunotherapy and vaccine development. Therefore, for examining the applicability of our glyco-NPs in the complex processes, dissociation of glyco-NPs in acidic organelles is a prerequisite for the antigen release and presentation process. To this goal, colocalization of glyco-NPs in DCs was performed first, then FRET ratio of the glyco-NPs changed in vitro was monitored for evaluating their possible dissociation. Both of the two important experiments were performed under a confocal fluorescent microscope.

Glyco-NPs were first proved with low cytotoxicity in vitro (Figure S18, Supporting Information). Thus a typical DC cell line, DC2.4 cells were incubated with **M-Man** or **M-Gal** for 4 h at 37 °C. After removal of the unbound glyco-NPs, fluorescence imaging of cells was carried out using confocal microscopy. To confirm that the uptake was resulted from specific interactions between sugars and receptors on cell surface, the cells were treated with competitive inhibitors, i.e., **PMan** or **PGal**, for 1 h prior to the incubation with the glyco-NPs. This resulted in significant inhibition of the endocytosis (Figure S19, Supporting Information).

As previously shown in literature,[13,5d] receptor-mediated endocytosis always follows the pathway from early endosome to late endosome and then to lysosome. The internalization pathways of **M-Man** and **M-Gal** in DCs were examined after endocytosis. To track this pathway, CellLight Early Endosomes-RFP BacMam 2.0 and CellLight Late Endosomes-RFP BacMam 2.0 for red fluorescence protein (RFP) expression were used to specifically label early endosome and late endosome, respectively; while LysoTracker Red DND-99 was used to label lysosome. In the confocal microscopy images of **M-Gal** (**Figure 2**), colocalization of green from the nanoparticle (first row) and red from early endosome, late endosome or lysosome (second row), was clearly evidenced by the yellow color in the merged images (third and fourth row). Similarly, colocalization of **M-Man** with the three acidic organelles was also observed (Figure 2). From the dominant yellow color in the third and fourth row, one may conclude that almost all of the glyco-NPs followed the classical pathway and existed either in early endosome, later endosome, or in lysosome. This of course makes the subsequent pH-responsive dissociation of glyco-NPs in vitro possible.

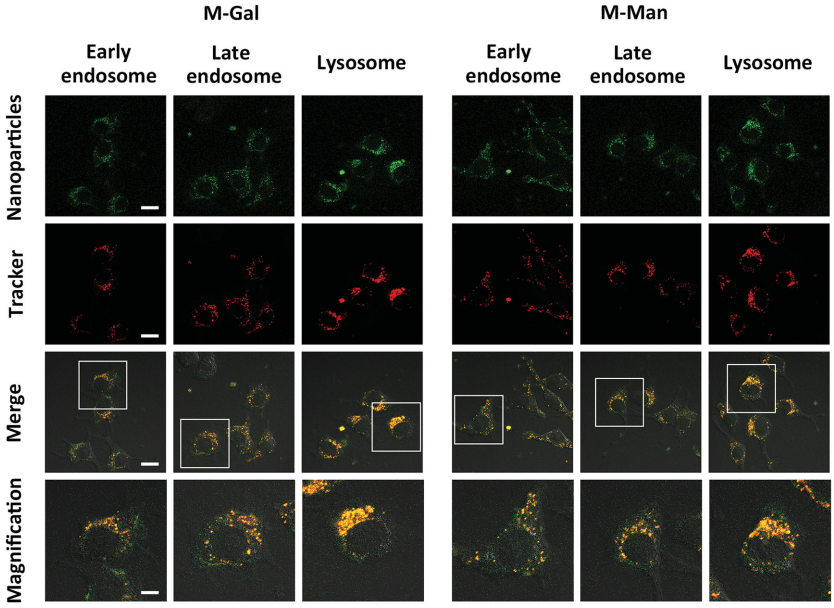

Figure 2. Localization of **M-Man** and **M-Gal** (with only NBD group) with early endosome, late endosome, lysosome. DC2.4 cells were incubated with **M-Gal** and **M-Man** for 4 h at 37 °C. Confocal images of DC2.4 cells show intracellular location of nanoparticles in green, CellLight BacMam labeling early and late endosomes and LysoTracker labeling lysosomes in red, and merged image in yellow (scale bar in the row of nanoparticles, tracker and merge: 10 μm; scale bar in the magnification row: 25 μm).

small 2015,
DOI: 10.1002/smll.201501871

small NANO MICRO

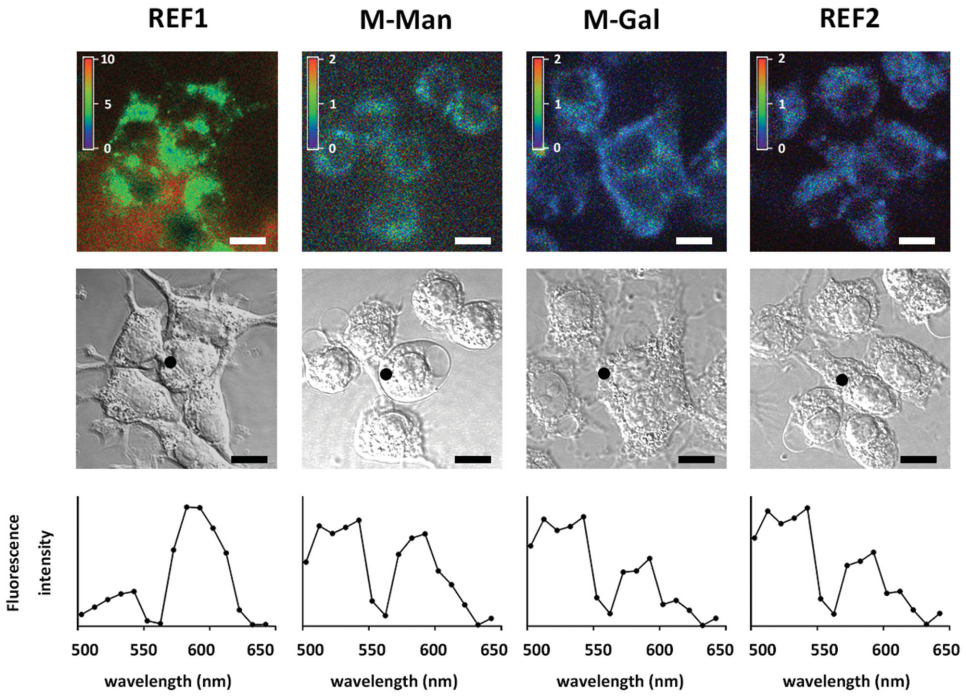

Figure 3. Images of confocal fluorescent microscope for DC2.4 cells incorporated with samples **REF1**, **M-Gal**, **M-Man**, and **REF2**. First row: Color in cells represents the FRET ratio as indicated in the bar; second row: cell images under bright field (scale bar: 10 μm); third row: FRET-induced fluorescence detected in ROI. Excitation: 488 nm, emission spectrum profile: 500–650 nm.

Measuring the FRET ratio change in vitro is not as straightforward as that in buffer. First, we need appropriate references to present *standard* FRET when they are incorporated in DCs. Herein, we designed two references. **REF1**, was a stable micelle with a "constant" FRET feature. The micelle was composed of two block copolymers (PNIPAm-co-NBD)-*b*-PBob and (PNIPAm-co-RhB)-*b*-PBob (weight ratio: 4:1), which share the same backbone but carrying NBD and RhB, respectively, in the first block (structures in detail and characterization are in Scheme S4 and Figure S20, Supporting Information). Due to the hydrophilicity of the first block and hydrophobicity of the second block, the copolymers self-assembled into common micelles. FRET ratio of the **REF1** micelle in solution was around 5.0, similar to the highest FRET ratio of glyco-NPs. As expected, because formation of the micelles was caused by amphiphilicity, regardless of the dynamic covalent bonding, they showed complete stability to either temperature or pH. That is what we observed by FRET of **REF1** in buffer (Figure S21, Supporting Information), which indicated that the measured FRET ratio of **REF1** could be regarded as a hallmark of complete chain association of glyco-NPs in DCs. On the other hand, **REF2**, formed by **N-PBOB** and **PGal** (weight ratio: 1:1) without acceptor **R-PGal** can be regarded as a representative of a totally disassociated one. To explore the performance of the glyco-NPs in the three acidic organelles, confocal FRET analysis on the nanoparticles and the reference samples inside DCs were carried out. DC2.4 cells were seeded on culture dishes at a concentration of 10^5 cells per dish, and cultured overnight. Then the cells were treated respectively with **M-Gal** and **M-Man** with an original FRET ratio around 2.0 for 4 h at 37 °C. Meanwhile, the cells were treated with **REF1** and **REF2** separately under the same condition. Then the cells were washed with PBS buffer, and fixed with 4% paraformaldehyde for 10 min. Confocal images and FRET signals of the cells were observed under Nikon C2+ confocal microscope with excitation wavelength at 488 nm.

As shown in **Figure 3**, the color observed in DCs directly presented the FRET effect and meanwhile the average FRET ratio, I_{587}/I_{538} was calculated. **REF1** gave the highest FRET ratio (≈5.0, in yellow), while those of **M-Gal** and **M-Man** were lower than 2.0. This dramatic difference clearly demonstrated the dissociation of glyco-NPs in DCs. However, the FRET ratio of **M-Man** (≈1.0, in cyan) was larger than that of **M-Gal** (≈0.4, in blue), indicating a less degree of dissociation for the former than the later. This is consistent to that obtained in buffer. Moreover, the dissociation of **M-Gal** is almost complete as it showed the same color as that from **REF2**, which did not contain a FRET effect. And the color of **M-Man** is between that of **REF1** and **M-Gal** as a result of its partial dissociation. The fluorescent spectroscopy (the bottom row in Figure 3) of ROI (region of interest, the black dot in the second row) inside DCs confirmed the FRET effect indicated in color.

In short, by combining the result of colocalization and pH-responsive property of glyco-NPs in DCs, we may conclude that both of glyco-NPs dissociated in DCs, which was induced by the low pH of acidic organelles at the incubation temperature 37 °C. To our best knowledge, the study on precise localization and characterization of stimuli-responsive dissociation of polymeric nanoparticles through the endocytic pathway has not been reported in literature. Dissociation of glyco-NPs via this pathway provides valuable information for their further application as antigen carrier.

DOI: 10.1002/smll.201501871

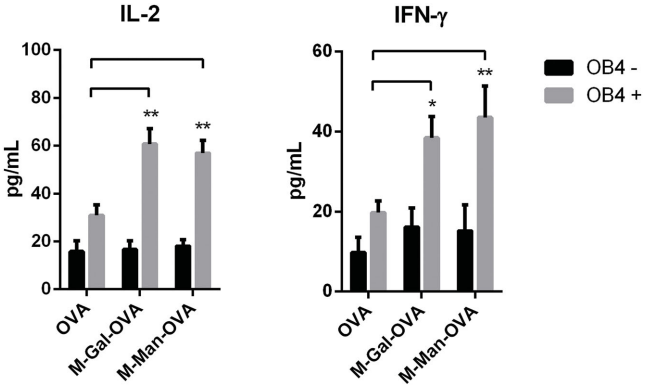

Figure 4. DC2.4 cells were incubated with OVA and OVA-loaded glyco-NPs (M-Gal-OVA and M-Man-OVA) for 4 h following 10 ng mL^{-1} IFN-γ treatment. Then OVA-loaded DC2.4 cells were coincubated with (OB4+) or without (OB4-) OB4 cells (OVA266–277 specific) for 48 h. Supernatant was collected for IL-2 and IFN-γ analysis by ELISA. Student's t-test. Values presented as mean ± SEM. $*p < 0.05$, $**p < 0.01$.

2.5. Antigen Presentation of OVA-Loaded Glyco-NPs to T Cells

It is known that antigen presentation is a vital process of immune system. It participates in various immune processes, including activating T helper cell and cytotoxic T cell killing. It is currently believed that extremely potent T-cell responses will be required to treat diseases such as acquired immune deficiency syndrome (AIDS) and cancer.[14] In our study, antigen presentation assays were performed to test the role and efficiency of the glyco-NPs. As a model antigen, OVA was encapsulated in glyco-NPs (encapsulation efficiency in the Supporting Information). The responses of a T cell line, $OVA_{266–277}$ specific OB4 cells were used as effecter cells, which indicate the efficiency of OVA presentation by DCs. DC2.4 cells were first treated with 10 ng mL^{-1} IFN-γ overnight for full maturation. Then they were incubated with OVA-loaded glyco-NPs for 4 h followed by washing with PBS buffer. Afterward, the OVA-loaded DC2.4 cells were cocultured with or without two times OB4 cells for 48 h. The supernatant was collected for Interleukin 2 (IL-2) and Interferon gamma (IFN-γ) detection by enzyme-linked immunosorbent assay (ELISA). As shown in **Figure 4**, compared with free OVA group and the control group without OB4 cells (OB4-), OVA loaded in glyco-NPs induced a significant increase of IL-2 and IFN-γ secretion by OB4 cells, which could be attributed to the enhanced antigen processing and presentation. This result highlights the effective protection as well as controllable release of glyco-NPs for the antigens, which may contribute to the further studies on their applications in cancer immunotherapy and vaccine development.

Supporting Information

Supporting Information is available from the Wiley Online Library or from the author.

Acknowledgements

Ministry of Science and Technology of China (2011CB932503), National Natural Science Foundation of China (Nos. 21474020, 91227203, 51322306, and GZ962), and the Innovation Program of the Shanghai Municipal Education Commission are acknowledged for their financial support.

[1] Y. Zhao, F. Sakai, L. Su, Y. Liu, K. Wei, G. Chen, M. Jiang, *Adv. Mater.* **2013**, *25*, 5215.
[2] a) M. Marguet, C. Bonduelle, S. Lecommandoux, *Chem. Soc. Rev.* **2013**, *42*, 512; b) M. Marguet, L. Edembe, S. Lecommandoux, *Angew. Chem. Int. Ed.* **2012**, *51*, 1173.
[3] a) Q. Zhang, L. Su, J. Collins, G. Chen, R. Wallis, D. A. Mitchell, D. M. Haddleton, C. R. Becer, *J. Am. Chem. Soc.* **2014**, *136*, 4325; b) M. W. J. L. Otten, S.-J. Richards, R. Lowery, D. J. Philips, D. M. Haddleton, M. I. Gibson, *Chem. Sci.* **2014**, *5*, 1611; c) A. Dag, J. C Zhao, M. H. Stenzel, *ACS Macro Lett.* **2015**, *4*, 579; d) R. Okoth, A. Basu, *Beilstein J. Org. Chem.* **2013**, *9*, 608.
[4] a) M. J. Mouw, K. Godula, J. E. Hudak, J. N. Lakins, A. C. Wijekoon, L. Cassereau, M. G. Rubashkin, M. J. Magbanua, K. S. Thorn, M. W. Davidson, H. S. Rugo, J. W. Park, D. A. Hammer, G. Giannone, C. R. Bertozzi, V. M. Weaver, *Nature* **2014**, *511*, 319; b) J. E. Hudak, S. M. Canham, C. R. Bertozzi, *Nat. Chem. Biol.* **2014**, *10*, 69.
[5] J. Huang, C. Bonduelle, J. Thévenot, S. Lecommandoux, A. Heise, *J. Am. Chem. Soc.* **2012**, *134*, 119; b) L. Su, Y. Zhao, G. Chen, M. Jiang, *Polym. Chem.* **2012**, *3*, 1560; c) S. de Medeiros, I. Otsuka, S. Fort, E. Minatti, R. Borsali, S. Halila, *Biomacromolecules* **2012**, *13*, 1129; d) P. Sun, Y. He, M. Lin, Y. Zhao, Y. Ding, G. Chen, M. Jiang, *ACS Macro Lett.* **2014**, *3*, 96; e) G. Pasparakis, C. Alexander, *Angew. Chem. Int. Ed.* **2008**, *47*, 4847.
[6] L. Su, W. Zhang, X. Wu, Y. Zhang, X. Chen, G. Liu, G. Chen, M. Jiang, *Small* **2015**, 33, 4191.
[7] a) Y. Kotsuchibashi, R. V. C. Agustin,. J.-Y. Lu, D. G. Hall, R. Narain, *ACS Macro Lett.* **2013**, *2*, 260; b) C. C. Deng, W. L. A. Brooks, K. A. Abboud, B. S. Sumerlin, *ACS Macro Lett.* **2013**, *2*, 220; c) L. X. Li, Z. W. Bai, P. A. Levkin, *Biomaterials.* **2013**, *34*, 8504; d) H. Yang, X. H. Sun, G. Liu, R. J. Ma, Z. Li, Y. L. An, L. Q. Shi, *Soft Matter* **2013**, *9*, 8589.
[8] a) M. Bérubé, M. Dowlut, D. G. Hall, *J. Org. Chem.* **2008**, *73*, 6471; b) H. Kim, Y. J. Kang, S. Kang, K. T. Kim, *J. Am. Chem. Soc.* **2012**, *134*, 4030.
[9] M. Lin, P. Sun, G. Chen, M. Jiang, *Chem. Commun.* **2014**, *50*, 9779.
[10] M. Jiang, M. Li, M. Xiang, H. Zhou, *Adv. Polym. Sci.* **1999**, *146*, 121.
[11] a) D. Wang, T. Liu, J. Yin, S. Y. Liu, *Macromolecules.* **2011**, *44*, 2282; b) X. Wan, S. Y. Liu, *J. Mater. Chem.* **2011**, *21*, 10321.
[12] B. Halliwell, M. V. Clement, L. H. Long, *FEBS Lett.* **2000**, *486*, 10.
[13] A. Varki, R. D. Cummings, J. D. Esko, H. H. Freeze, *Essentials of Glycobiology*, 2nd ed., Cold Spring Harbor, NY **2009**.
[14] J. J. Moon, H. Suh, A. Bershteyn, M. T. Stephan, H. Liu, *Nat. Mater.* **2011**, *10*, 243.

Received: June 26, 2015
Revised: August 27, 2015
Published online:

DOI: 10.1002/smll.201501871